Contributed paper

OPTO-ELECTRONICS REVIEW **13**(1), 51–60

Diagonal relations between elegant Hermite-Gaussian and Laguerre-Gaussian beam fields

Y. PAGANI and W. NASALSKI*

Institute of Fundamental Technological Research, Polish Academy of Sciences
Świętokrzyska Str. 21, 00-049 Warsaw, Poland

Standard Hermite-Gaussian and standard Laguerre-Gaussian diagonal beams can be expressed by similar summation of non-diagonal standard Hermite-Gaussian beams with expansion coefficients that are equal in magnitude in both cases. We show theoretically and numerically that the same relations hold also for elegant Hermite-Gaussian beams and elegant Laguerre-Gaussian beams. On the other hand, our theoretical estimations and numerical simulations show substantial differences between standard and elegant beams in their phase transverse distribution and evolution of this distribution during beam propagation.

Keywords: optical beams, singular optics, phase singularities.

1. Introduction

Hermite-Gaussian (HG) and Laguerre-Gaussian (LG) beams are higher order solutions of the paraxial wave equation with rectangular and cylindrical symmetry about their axes of propagation, respectively. They are widely used in the theory of laser beams and resonators [1,2]. When arguments in Hermite or Laguerre parts of these beam fields are real and arguments in Gaussian parts are complex, they are named Standard Hermite-Gaussian (SHG) or Standard Laguerre-Gaussian (SLG) beams. Siegman found more symmetric solutions where both arguments in the Gaussian and the Hermite (Laguerre) parts are the same complex quantity, and he named them Elegant Hermite-Gaussian (EHG) and Elegant Laguerre-Gaussian (ELG) beams [2,3]. After Siegman's work, Pratesi and Ronchi derived a more general complex Gaussian solution that can be reduced to SHG or EHG beams [4]. Elegant and standard HG and LG beams exhibit several different features during propagation. For example, EHG beams have no spherical wavefronts, have no zeroes outside their waists for odd orders of Hermite functions, are much more concentrated around the beam axis in near field and their outermost side-lobes become strongly emphasised in far field [2,5].

The SHG and SLG beams form complete sets in the space of square-integrable complex functions. Any finite power beam solution of the paraxial wave equation can be decomposed in these bases. That means that also the SLG beams can be expressed by series of the SHG beams and vice-versa. In particular, a diagonal SHG beam, that is the three-dimensional (3D) beam symmetry axes of which, say x' and y' axes, make an angle of $\pi/4$ with respect to the assumed coordinate axes x and y of an optical system, can be expressed by summation of non-diagonal SHG beams, that is the SHG beams factored out into two-dimensional (2D) HG beams along the x and y axes, respectively. Almost the same expansion is valid for SLG beams, except additional factors of $-i$ present in coefficients of this expansion [6,7]. For example, a diagonal SHG_{01} beam can be expressed as

$$SHG_{01}(x',y',z') = 2^{-1/2}[SHG_{10}(x,y,z) + SHG_{01}(x,y,z)] \propto x'G(x,y,z),$$

where $G(x,y,z)$ is a fundamental Gaussian mode, $x' = (x + y)/\sqrt{2}$ and $y' = (x - y)/\sqrt{2}$. Similarly a SLG_{01} beam is given by

$$SHG_{01}(r,\varphi,z) = 2^{-1/2}[SHG_{10}(x,y,z) + iSHG_{01}(x,y,z)] \propto x''G(x,y,z),$$

where $x'' = (x + iy)/\sqrt{2} = r\exp(+i\varphi)$ and $y'' = (x - iy)/\sqrt{2} = r\exp(-i\varphi)$. The diagonal x' and y' coordinates are obtained by rotation of the (non-diagonal) x and y axes through the real angle $\pi/4$ whereas the circular (or imaginary diagonal) x'' and y'' coordinates may by understood as given by rotation of the x and y axes through the imaginary angle $\pi/4$. The elegant and standard beams of first two orders ($n, m = 0,1$) are indistinguishable from each other [2,5]. In the case of the first-order Hermite-Gaussian beams, for example, they correspond to a product of Gaussian function with one coordinate variable: x or y. Consequently, the two previous relations given for standard beams remain also valid for elegant beams of these two first orders. In fact, as we will show in this communication, these relations still remain valid for EHG and ELG beams of any order.

*e-mail: wnasal@ippt.gov.pl

The above formulas are not only nice and compact mathematical expressions but also of, both theoretical and experimental, important physical consequences. In 1992, Allen and coworkers have shown that a SLG beam posses well-defined orbital angular momentum [7]. It causes notably mechanical effects, like rotation, already presented in experiments with optical spanners. Its interaction with matter is also involved in other phenomena, like the second – harmonic generation in non-linear optics [8]. Therefore, studies on properties of the SLG beams, their generation, propagation, and various applications are of great importance. Many aspects of these phenomena need further explanation and are recently under active research. As Allen *et al*. pointed out: "It would be appear that all light beams which possess field gradients, and which are not therefore planes waves, will possess a measure of orbital angular momentum. Indeed a badly phased transformation between transverse laser amplitude distributions will in general lead to ill-defined orbital angular momentum. For this reason it is important that stable, nondegenerate, propagating Laguerre-Gaussian polynomial modes are created and entirely transformed. A meaningful measurement of orbital angular momentum will not otherwise result" [7].

The formulas similar to these outlined above permit one to produce astigmatic optical systems in order to convert (standard) Laguerre-Gaussian modes to (standard) Hermite-Gaussian modes or vice versa. That explains importance of such expressions. On the other hand, elegant beams have not been studied deeply and employed in this way yet. However, it is already known that they posses very interesting properties. For example, it has been shown that elegant beams possess a better M^2 beam propagation factor than this of standard beams [5,9]. For this reason elegant beams may appear to be more useful than standard beams in many future applications.

The paper is decomposed into three parts. First, we introduce basic notation and definitions for beams under consideration. Next, we recall known diagonal relations for standard beams, and give corresponding new relations for elegant beams. We also verify these relations numerically in several planes transverse to a propagation direction. Detailed analytic derivation of these relations are given in an appendix. Finally, we also show that differences in field phase distributions between two types of beams exist and that they are substantial.

2. Basic definitions

We consider time-harmonic beam fields propagating along the z-axis. A phase factor $\exp(i(kz - \omega t))$ is assumed and suppressed henceforth in all beam field expressions. The reduced coordinates: $\tilde{x} = x/w_0$, $\tilde{y} = y/w_0$, $\tilde{r} = r/w_0$, $\tilde{z} = z/z_0$, are used, where w_0 and $z_0 = kw_0^2/2$ are the characteristic width and characteristic (diffraction) length of a Gaussian beam, respectively. In these coordinates, the SHG and EHG beams are solutions of the 3D paraxial wave equation

$$\left(\frac{\partial^2}{\partial\tilde{x}^2}+\frac{\partial^2}{\partial\tilde{y}^2}+4i\frac{\partial}{\partial\tilde{z}}\right)\psi(\tilde{x},\tilde{y},\tilde{z})=0. \tag{1}$$

They are given in a form of the product of two 2D solutions in the two mutually orthogonal planes $(\tilde{x},\tilde{z})$ and $(\tilde{y},\tilde{z})$, respectively:

$$\psi_{nm}^{SHG}(\tilde{x},\tilde{y},\tilde{z})=2^{-\frac{n+m}{2}}\sqrt{\frac{2}{n!m!\pi}}\left(\frac{v(\tilde{z})^*}{v(\tilde{z})}\right)^{n+m} \times H_n\left(\frac{\sqrt{2}\tilde{x}}{w(\tilde{z})}\right)H_m\left(\frac{\sqrt{2}\tilde{y}}{w(\tilde{z})}\right)G(\tilde{x},\tilde{y},\tilde{z}), \tag{2}$$

$$\psi_{nm}^{EHG}(\tilde{x},\tilde{y},\tilde{z})=2^{-\frac{n+m}{2}}\sqrt{\frac{2}{n!m!\pi}}\left(\frac{1}{v(\tilde{z})}\right)^{n+m} \times H_n\left(\frac{\tilde{x}}{v(\tilde{z})}\right)H_m\left(\frac{\tilde{y}}{v(\tilde{z})}\right)G(\tilde{x},\tilde{y},\tilde{z}), \tag{3}$$

where $H_n(\tilde{x})$ and $H_m(\tilde{y})$ are Hermite polynomials of order n and m in $\tilde{x}$ and $\tilde{y}$ directions, respectively, and the symbol "*" denotes complex conjugate.

The real beam radius $w(\tilde{z})$, complex beam radius $v(\tilde{z})$, Guoy phase $\zeta(\tilde{z})$ and the fundamental Gaussian beam $G(\tilde{x},\tilde{y},\tilde{z})$ are defined as

$$w(\tilde{z})=\sqrt{1+\tilde{z}^2}, \tag{4}$$

$$v(\tilde{z})=\sqrt{1+i\tilde{z}}, \tag{5}$$

$$\zeta(\tilde{z})=\arctan(\tilde{z}), \tag{6}$$

$$G(\tilde{x},\tilde{y},\tilde{z})=v^{-2}(\tilde{z})e^{-(\tilde{x}^2+\tilde{y}^2)/v^2(\tilde{z})}. \tag{7}$$

Note that both HG beams are normalized in power, their field amplitudes are equal at their waist centers. Both beams are uniquely determined by magnitudes of the rectangular coordinates and the complex radius $v(\tilde{z})$ of the beams.

Counterparts of the Hermite-Gaussian beams, these with cylindrical symmetry in beam-field intensity, are the standard SLG and elegant ELG Laguerre-Gaussian beams. They are solutions of the paraxial wave equation in the cylindrical coordinates $(\tilde{r},\varphi,\tilde{z})$

$$\left(\frac{1}{\tilde{r}}\frac{\partial}{\partial\tilde{r}}\left(\tilde{r}\frac{\partial}{\partial\tilde{r}}\right)+\frac{1}{\tilde{r}^2}\frac{\partial^2}{\partial\varphi^2}+4i\frac{\partial}{\partial\tilde{z}}\right)\Phi(\tilde{r},\varphi,\tilde{z})=0, \tag{8}$$

where φ denotes an azimuthal angle in the plane $(\tilde{x},\tilde{y})$ transverse to the propagation direction. In the notation of Beijersbergen *et al*. [10] the SLG and ELG beams can be written as

$$\Phi_{nm}^{SLG}(\tilde{r},\varphi,\tilde{z})=\sqrt{\frac{2}{\pi n!m!}}(-1)^{\min(n,m)}\min(n,m)!\left(\frac{v(\tilde{z})^*}{v(\tilde{z})}\right)^{n+m} \times\left(\frac{\sqrt{2}\tilde{r}}{w(\tilde{z})}\right)^{|n-m|}L_{\min(n,m)}^{|n-m|}\left(\frac{2\tilde{r}^2}{w^2(\tilde{z})}\right)G(\tilde{x},\tilde{y},\tilde{z})e^{i(n-m)\varphi} \tag{9}$$

$$\Phi_{nm}^{ELG}(\tilde{r},\varphi,\tilde{z})=\sqrt{\frac{2}{n!m!\pi}}(-1)^{\min(n,m)}\min(n,m)!\left(\frac{1}{v(\tilde{z})}\right)^{n+m} \times\left(\frac{\tilde{r}}{v(\tilde{z})}\right)^{|n-m|}L_{\min(n,m)}^{|n-m|}\left(\frac{\tilde{r}^2}{v^2(\tilde{z})}\right)G(\tilde{x},\tilde{y},\tilde{z})e^{i(n-m)\varphi} \quad (10)$$

respectively, where $L_{\min(n,m)}^{|n-m|}$ are the generalized Laguerre polynomials. The indices n and m are related to the usual radial p and azimuthal l indices by the relations: $p = \min(n,m)$ and $l = |n - m|$ [10]. The LG beams are also normalized in power, their field amplitudes are equal at their waist centers and are uniquely determined by magnitudes of the cylindrical coordinates and the complex radius $v(\tilde{z})$ of the beams.

Figures 1 and 2 represent the transverse intensity distribution of the SHG, SLG, EHG and ELG beam fields in one transverse dimension at the beam waist ($\tilde{z} = 0$). In spite of the visible analytic similarity between standard and elegant beams, they behave differently due to the complex argument in elegant beams expressions: for example, EHG and ELG beams exhibit changes of shape during the propagation and they do not have spherical wavefronts. Comparisons between elegant and standard beams by use of different criteria, like, for example, the quality factor or the kurtosis parameter, have already been done by several authors [5,11,12].

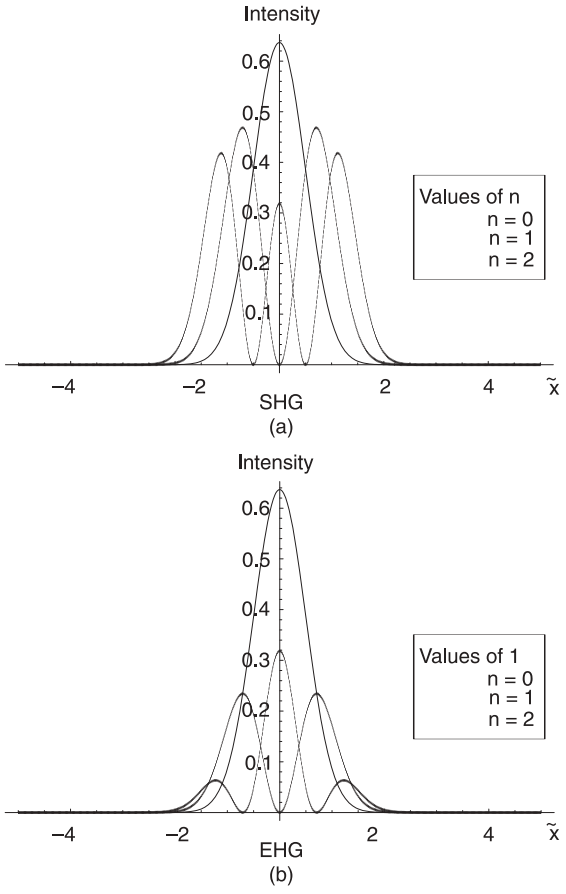

Fig. 1. Intensity of the fundamental $n = 0$, first-order $n = 1$ and second-order $n = 2$ SHG and EHG beams versus the reduced coordinate $\tilde{x}$ for different values of n at the beam waist ($\tilde{z} = 0$).

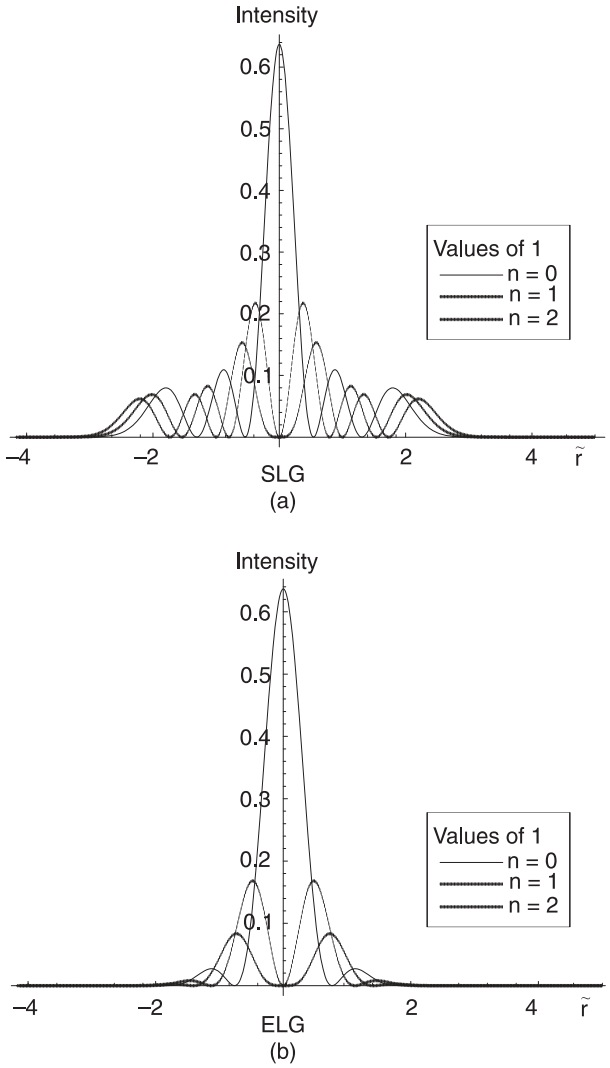

Fig. 2. Intensity of SLG and ELG beams as a function of the reduced $\tilde{r}$ coordinate for different values of l and for $p = 2$ at the beam waist ($\tilde{z} = 0$).

3. Diagonal relations between beam fields

It has been previously shown [6,7,10] that the diagonal – SHG beam, that is the SHG beam rotated by an angle of $\pi/4$ from its cartesian reference coordinates $\tilde{x}$ and $\tilde{y}$, can be expressed by a summation of non-rotated SHG beams, where successive components of this summation are in phase. Similarly, the SLG beam can be decomposed into a sum a non-rotated SHG beams, where the summation components of the same magnitude are augmented by additional $-\pi/2$ phase factors

$$\Psi_{nm}^{SHG}\left(\frac{\tilde{x}-\tilde{y}}{\sqrt{2}},\frac{\tilde{x}+\tilde{y}}{\sqrt{2}},\tilde{z}\right)=\sum_{k=0}^{n+m}b(n,m,k)\Psi_{n+m-k,k}^{SHG}(\tilde{x},\tilde{y},\tilde{z}), \quad (11)$$

$$\Phi_{nm}^{SLG}(\tilde{r},\varphi,\tilde{z})=\sum_{k=0}^{n+m}(-i)^k b(n,m,k)\Psi_{n+m-k,k}^{SHG}(\tilde{x},\tilde{y},\tilde{z}). \quad (12)$$

Real coefficients in these expansions

$$b(n,m,k) = \sqrt{\frac{(n+m-k)!\,k!}{n!\,m!\,2^{n+m}}}(-2)^k P_k^{(n-k,m-k)}(0), \quad (13)$$

are expressed by the Jacobi polynomials [6]

$$P_k^{(\nu,\mu)}(t) = \frac{(-1)^k}{2^k\,k!}(1-t)^{-\nu}(1+t)^{-\mu} \times \frac{d^k}{dt^k}\left[(1-t)^{k+\nu}(1+t)^{k+\mu}\right] \quad (14)$$

A graphical illustration of these formulas is given in Fig. 3, where transverse cross-sections of the second order beams with $n = 2$ and $m = 0$ are drawn at the beam waists.

Comparing the expansions in Eqs. 11 and 12 we can see that except the factor $(-i)^k$ their coefficients are equal. The factor $(-i)^k$ corresponds physically to an additional change of phase $-k\pi/2$ for each integer k. Compensation of this phase by Guoy phase $\zeta(\tilde{z})$ of an astigmatic HG beam, that is the beam with different diffraction lengths z_{0x} and z_{0y} with respect to its symmetry axes x and y, respectively, leads to mode conversion between the incoming SHG beam and the outgoing SLG beam or, inversely, between the incoming SLG beam and the outgoing SHG beam. Moreover, contrary to the SHG beams, the SLG beams possess an angular momentum of magnitude $l\hbar$ per photon, where $l = n - m$ stands for the azimuthal index of SLG beam. Thus the transformation of the SHG beam into the SLG beam or vice-versa causes the beam field to exert a torque on the converter. This type of mode converter, that is the $\pi/2$ – converter, has been discussed in deep by several authors [6,7,10].

Zauderer and Takenaka *et al*. have obtained some relations between EHG and ELG beams [13,14] in their analyzes of beam fields beyond the paraxial approximation; see, for example, a formula (31) in Ref. [14]. To our best knowledge, diagonal relations for elegant beams, parallel to the equations (11) and (12) for standard beams, have not been given as yet. However it is directly proved in Appendix that identical diagonal relations really hold also for elegant beams

$$\Psi_{nm}^{EHG}\left(\frac{\tilde{x}-\tilde{y}}{\sqrt{2}}, \frac{\tilde{x}+\tilde{y}}{\sqrt{2}}, \tilde{z}\right) = \sum_{k=0}^{n+m} b(n,m,k)\Psi_{n+m-k,k}^{EHG}(\tilde{x},\tilde{y},\tilde{z}), \quad (15)$$

$$\Phi_{nm}^{ELG}(\tilde{r},\varphi,\tilde{z}) = \sum_{k=0}^{n+m}(-i)^k\, b(n,m,k)\Psi_{n+m-k,k}^{EHG}(\tilde{x},\tilde{y},\tilde{z}). \quad (16)$$

Therefore, the diagonal expansions of the standard (eq. 11 and eq. 12) and elegant (eq. 15 and eq. 16) HG or LG beams possess exactly the same expansion coefficients. In Fig. 4 a graphical representation of the formulas (15) and (16) is drawn at the waist of beams.

Since the shape of elegant beams changes during their propagation, it is not obvious from first sight that the diagonal relations for elegant beams remain valid when the propagation distance $\tilde{z}$ from the beam waist varies. Therefore, we have verified in addition numerically that the equations (15) and (16) were really valid even when $\tilde{z} \neq 0$. The case where $\tilde{z} = 1$ was considered as an example. We have computed the right hand-side of Eqs. 15 and 16 and compared the outcome with the definition of the left-hand part of these equations. Eq. 15 and eq. 16 remain valid in this case as expected. The cases of $n = 2$ and $m = 0$ for EHG and ELG are represented Fig. 5.

For better visualization, we have represented in Fig. 6 transverse one dimensional (1D) cross-sections of the beams in the cases drawn previously in Figs. 4(a) and 5(a). Moreover, we have also used Mathematica in order to check analytically Eqs. 11–12 and 15–16 for various n, m and $\tilde{z}$. We observed that the above relations appeared to be

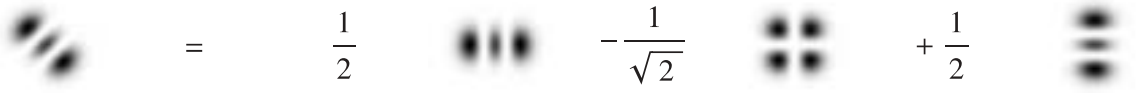

$$\Psi_{20}^{SHG}\left(\tfrac{\tilde{x}-\tilde{y}}{\sqrt{2}}, \tfrac{\tilde{x}+\tilde{y}}{\sqrt{2}}\right) = \tfrac{1}{2}\Psi_{20}^{SHG}(\tilde{x},\tilde{y}) - \tfrac{1}{\sqrt{2}}\Psi_{11}^{SHG}(\tilde{x},\tilde{y}) + \tfrac{1}{2}\Psi_{02}^{SHG}(\tilde{x},\tilde{y})$$

(a)

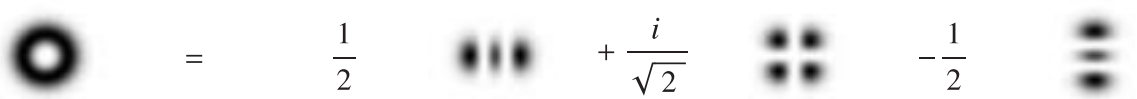

$$\Phi_{20}^{SLG}(\tilde{r},\varphi) = \tfrac{1}{2}\Psi_{20}^{SHG}(\tilde{x},\tilde{y}) + \tfrac{i}{\sqrt{2}}\Psi_{11}^{SHG}(\tilde{x},\tilde{y}) - \tfrac{1}{2}\Phi_{02}^{SHG}(\tilde{x},\tilde{y})$$

(b)

Fig. 3. Decomposition of the SHG Ψ_{20}^{SHG} and the SLG Φ_{20}^{SLG} diagonal beam fields in terms of the SHG beam fields in the transverse plane at the beam waist ($\tilde{z} = 0$).

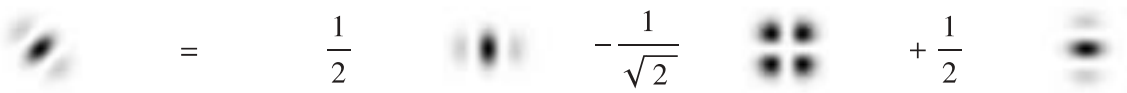

$$\Psi_{20}^{EHG}\left(\tfrac{\tilde{x}-\tilde{y}}{\sqrt{2}},\tfrac{\tilde{x}+\tilde{y}}{\sqrt{2}}\right)=\tfrac{1}{2}\Psi_{20}^{EHG}(\tilde{x},\tilde{y})-\tfrac{1}{\sqrt{2}}\Psi_{11}^{EHG}(\tilde{x},\tilde{y})+\tfrac{1}{2}\Psi_{02}^{EHG}(\tilde{x},\tilde{y})$$

(a)

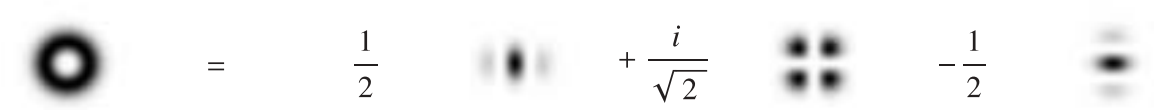

$$\Phi_{20}^{ELG}(\tilde{r},\varphi)=\tfrac{1}{2}\Psi_{20}^{EHG}(\tilde{x},\tilde{y})+\tfrac{i}{\sqrt{2}}\Psi_{11}^{EHG}(\tilde{x},\tilde{y})-\tfrac{1}{2}\Psi_{02}^{EHG}(\tilde{x},\tilde{y})$$

(b)

Fig. 4. Decomposition of the EHG Ψ_{20}^{SHG} and the ELG Φ_{20}^{SLG} diagonal beam fields into a summation of EHG beams in the transverse plane at ($\tilde{z}=0$) (in the beam waist).

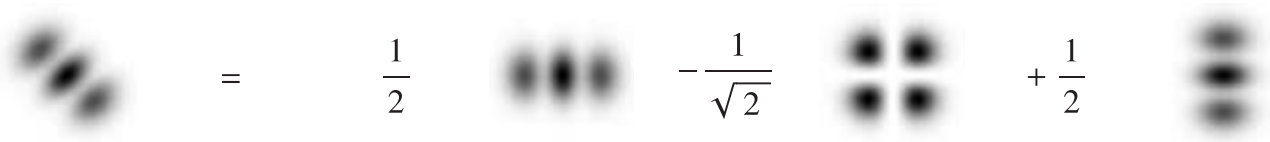

$$\Psi_{20}^{EHG}\left(\tfrac{\tilde{x}-\tilde{y}}{\sqrt{2}},\tfrac{\tilde{x}+\tilde{y}}{\sqrt{2}},\tilde{z}\right)=\tfrac{1}{2}\Psi_{20}^{EHG}(\tilde{x},\tilde{y},\tilde{z})-\tfrac{1}{\sqrt{2}}\Psi_{11}^{EHG}(\tilde{x},\tilde{y},\tilde{z})+\tfrac{1}{2}\Psi_{02}^{EHG}(\tilde{x},\tilde{y},\tilde{z})\ \text{with}\ \tilde{z}=1$$

(a)

$$\Phi_{20}^{ELG}(\tilde{r},\varphi,\tilde{z})=\tfrac{1}{2}\Psi_{20}^{EHG}(\tilde{x},\tilde{y},\tilde{z})+\tfrac{i}{\sqrt{2}}\Psi_{11}^{EHG}(\tilde{x},\tilde{y},\tilde{z})-\tfrac{1}{2}\Psi_{02}^{EHG}(\tilde{x},\tilde{y},\tilde{z})\ \text{with}\ \tilde{z}=1$$

(b)

Fig. 5. Decomposition of the EHG Ψ_{20}^{EHG} and the ELG Φ_{20}^{ELG} diagonal beam fields in terms of EHG beams in the transverse plane at ($\tilde{z}=1$) (outside the beam waist).

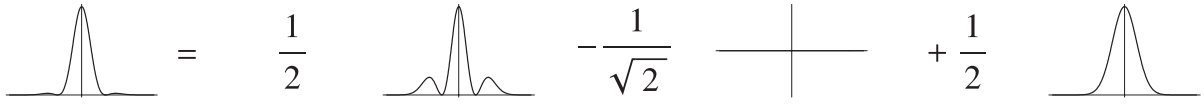

at $\tilde{z}=0$

(a)

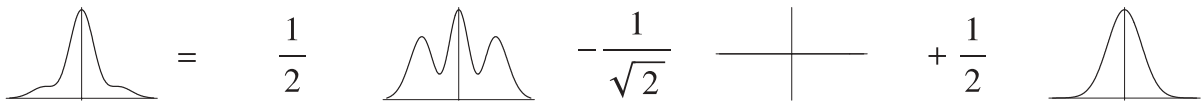

at $\tilde{z}=1$

(b)

Fig. 6. 1D cross-section ($\tilde{y}=0$) of the decomposition of the EHG beam Ψ_{20} at its waist (for ($\tilde{z}=0$) and outside its waist (for $\tilde{z}=1$). The coordinate crosses correspond to the function $f(x)=0$.

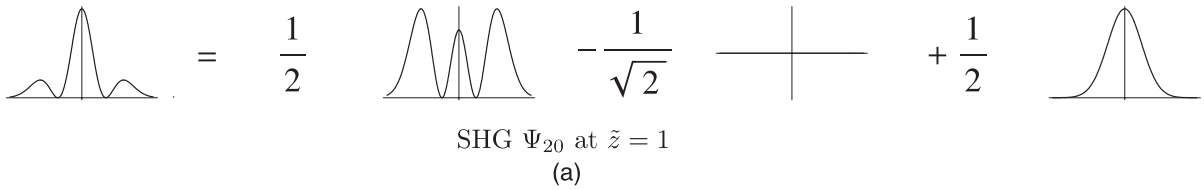

SHG Ψ_{20} at $\tilde{z} = 1$

(a)

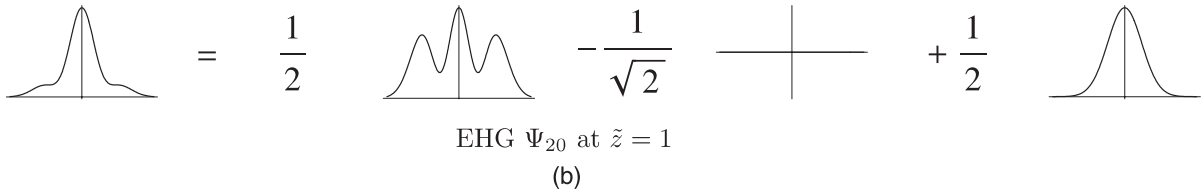

EHG Ψ_{20} at $\tilde{z} = 1$

(b)

Fig. 7. Graphical representation of Eq. (11) and Eq. (15) of the beam field distribution at $\tilde{z}$ = l; comparison of SHG and EHG beams by their 1D cross-sections at $\tilde{y} = 0$. The coordinate crosses represents the function $f(x) = 0$.

valid whatever values of n, m and $\tilde{z}$ may be. Finally, we enclose in Fig. 7 one example of comparison between the transverse shapes of field distributions of standard and elegant beams. The drawing indicates that the diagonal relations derived may have serious consequences of use of the elegant HG and LG beams in optical applications.

SLG and ELG beams share many common characteristics, one important example of them has been shown above by Eqs. (15) and (16). However, these beams exhibit also substantial differences, especially in their transverse field distribution and this field distribution changes in the course of beam propagation. Phase aspects of these differences will be briefly discussed in the next section.

4. Transverse distribution of beam field phase

A few papers have been published recently in which differences between standard and elegant Laguerre beams were discussed. Only intensity of beams has been considered in deep [5,9,11,12]. Therefore, we present here some further numerical results, pertaining phase distribution of beams and changes of this distribution during beam propagation.

In Figs. 8 and 9, we draw the phase transverse distribution of SLG and ELG beams. These figures show differences in beam phase distribution that appear to be present during the beam propagation from the beam waist plane ($\tilde{z} = 0$), through the Fresnel region, until the far-field range ($\tilde{z} = 10^4$). Different values of the beam orders n ($n = 2$ and $n = 5$) and m ($m = 1$ and $m = 2$) are considered. At first sight it may be surprising to observe that differences in phase distributions at their waists exist – at the waist SLG and ELG beam fields are purely real. However the jump which is observed for the beam field phase equals only π, that means that it only reverses signs of beam field amplitudes. Location of these phase discontinuities depend only on positions of zeroes of the Laguerre functions used in the description of the SLG and ELG beams. These zeroes are located at different transverse spatial points, for the difference in the scaling factors (by 2) present in their arguments. For example, in the case of n = 2 and m = 1, we use in our calculations at the beam waist plane the Laguerre function $L_1^1(\tilde{x},\tilde{y}) = 2 - (x^2 + y^2)$ for the ELG beam, and in the second case we use the Laguerre function $L_1^1(\tilde{x},\tilde{y}) = 2[1 - (x^2 + y^2)]$ of the different argument for the SLG beam. Zeros of these two functions are located on circles centered at $\tilde{x} = \tilde{y} = 0$ of radii $r = 1$ and $r = \sqrt{2}$, respectively. That explains changes in positions of the phase singularities of the circular form, as can be easily observed from the figures.

In general, except in the far-field region, the phase distributions of SLG and ELG beams and their phase differences may appear of very complicated form during the beam propagation. They depend on all the parameters of the beams (n,m,w,v,φ). Nevertheless, it can be observed that the beam phase distribution is smoother in the case of ELG beams than in the case of SLG beams. The SLG beams show more phase singularities during the beam propagation than the ELG beams do. Indeed, the SLG beams possess the additional phase jump of π due to the zeroes of the Laguerre function with a real agument, which does not exist for the ELG beams, where an argument of the Laguerre function is complex. For example, Fig. 8 shows the SLG beam field distribution, where the Laguerre function $L_1^1(\tilde{x},\tilde{y}) = 2[1 - (x^2 + y^2)/w^2(z)]$ is involved. Zeroes of this function are located on a circle centered at $\tilde{x} = \tilde{y} = 0$. A radius $r = w(z)$ of the circle increases with increase of the propagation distance, due to beam diffraction.

Finally it can be observed that in the far-field the beam field phase distributions become well defined, highly symmetric and clearly visible. The case of radial indices $n > m$ is considered; thus $m = \min(n,m)$ stands for the radial index of Laguerre functions describing the beams. Topological charges of the beam singularities are to equal $n - m$, that is to the number of the phase discontinuities or the phase jumps by π in the beam field transverse distribution. Locations of these phase discontinuities in the far field region depend only on the azimuthal angle φ and are different for the two different – standard and elegant – beam types. Differences of these locations are expressed uniquely by one parameter equal to $-m\pi/2 = -(\min(n, m))\ \pi/2$. It can be easily shown by taking the limit of the argument of equations Eqs. 9 and 10 when $\tilde{z}$ tends to infinity. We obtain in the case where $n > m$:

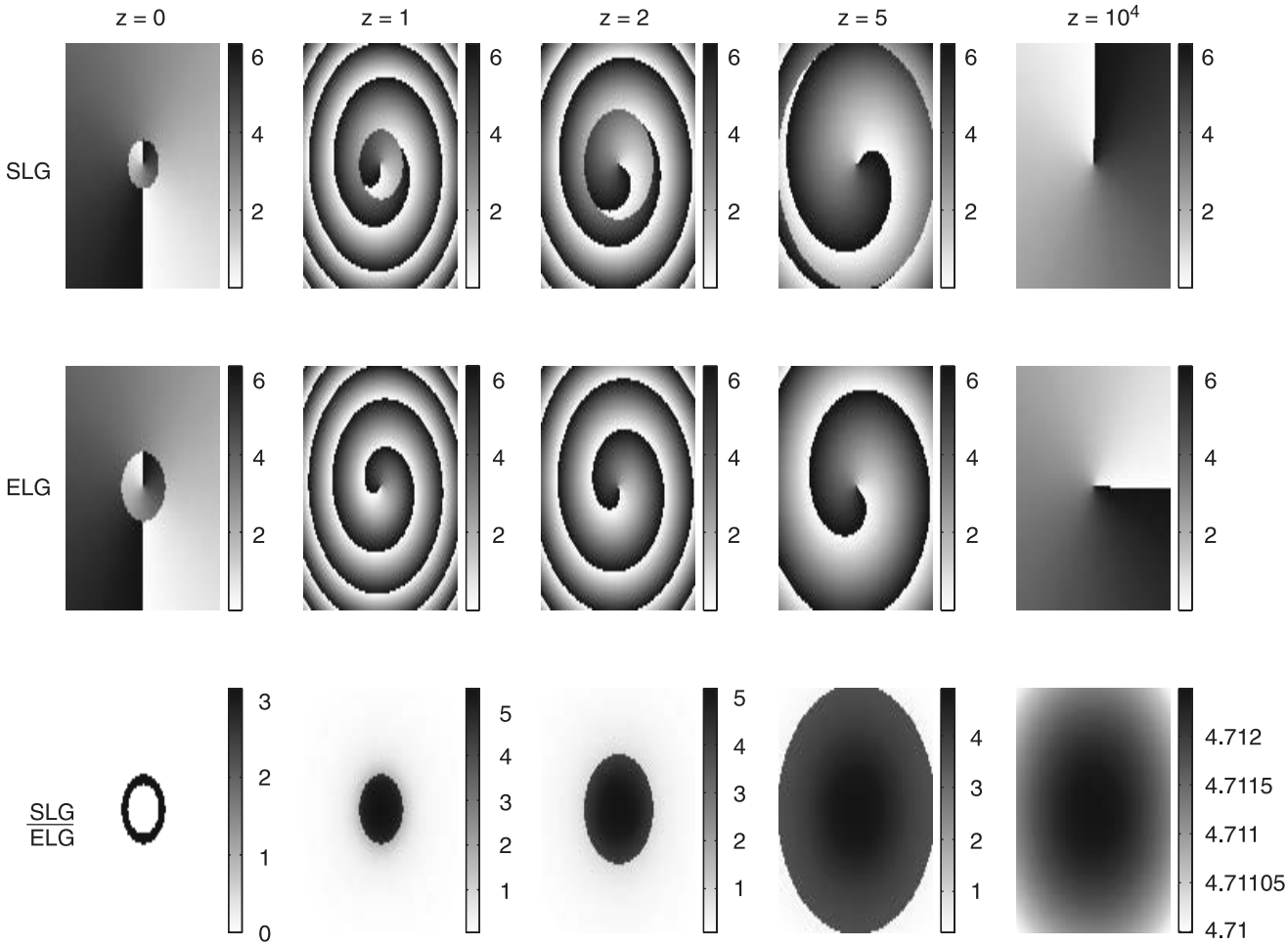

Fig. 8. Phase distribution in the transverse plane $(\tilde{x},\tilde{y})$ of $\phi_{nm}^{SLG}(\tilde{x},\tilde{y},\tilde{z})$ (first line), $\phi_{nm}^{ELG}(\tilde{x},\tilde{y},\tilde{z})$ (second line) and $\phi_{nm}^{SLG}(\tilde{x},\tilde{y},\tilde{z})/\phi_{nm}^{ELG}(\tilde{x},\tilde{y},\tilde{z})$ (third line) for $n = 2$, $m = 1$ at different $\tilde{z}$ positions: from the beam waist ($\tilde{z} = 0$) to the far-field ($\tilde{z} = 10^4$). We have set the argument to be between $[0,2\pi]$. For the first two lines, the white color stands for 0.

$$\arg_{SL} = \lim_{\tilde{z}\to\infty} \arg(\phi^{SLG}(\tilde{r},\varphi,\tilde{z})) = \lim_{\tilde{z}\to\infty} \arg\left(\sqrt{\frac{2}{\pi n!\,m!}}\min(n,m)!(-1)^{\min(n,m)}\right)$$
$$+ \arg(G(\tilde{x},\tilde{y},\tilde{z})) + \arg(e^{i(n-m)\varphi}) + \underbrace{\arg\left(L_{\min(n,m)}^{|n-m|}\left(\frac{2\tilde{r}^2}{w^2(\tilde{z})}\right)\right)}_{=0} + \arg\left((\sqrt{2}\tilde{r})^{|n-m|}\right)$$
$$+ \underbrace{\arg\left(\left(\frac{1}{w(\tilde{z})}\right)^{|n-m|}\right)}_{=0} + \underbrace{\arg\left(\left(\frac{v(\tilde{z})^*}{v(\tilde{z})}\right)^{n+m}\right)}_{-(n+m)\pi/2}$$

and

$$\arg_{EL} = \lim_{\tilde{z}\to\infty} \arg(\phi^{ELG}(\tilde{r},\varphi,\tilde{z})) = \lim_{\tilde{z}\to\infty} \arg\left(\sqrt{\frac{2}{\pi n!\,m!}}\min(n,m)!(-1)^{\min(n,m)}\right)$$
$$+ \arg(G(\tilde{x},\tilde{y},\tilde{z})) + \arg(e^{i(n-m)\varphi}) + \underbrace{\arg\left(L_{\min(n,m)}^{|n-m|}\left(\frac{\tilde{r}^2}{v^2(\tilde{z})}\right)\right)}_{=0} + \arg\left((\tilde{r})^{|n-m|}\right) + \underbrace{\arg\left(\left(\frac{1}{v(\tilde{z})}\right)^{2n}\right)}_{=-n\pi/2}.$$

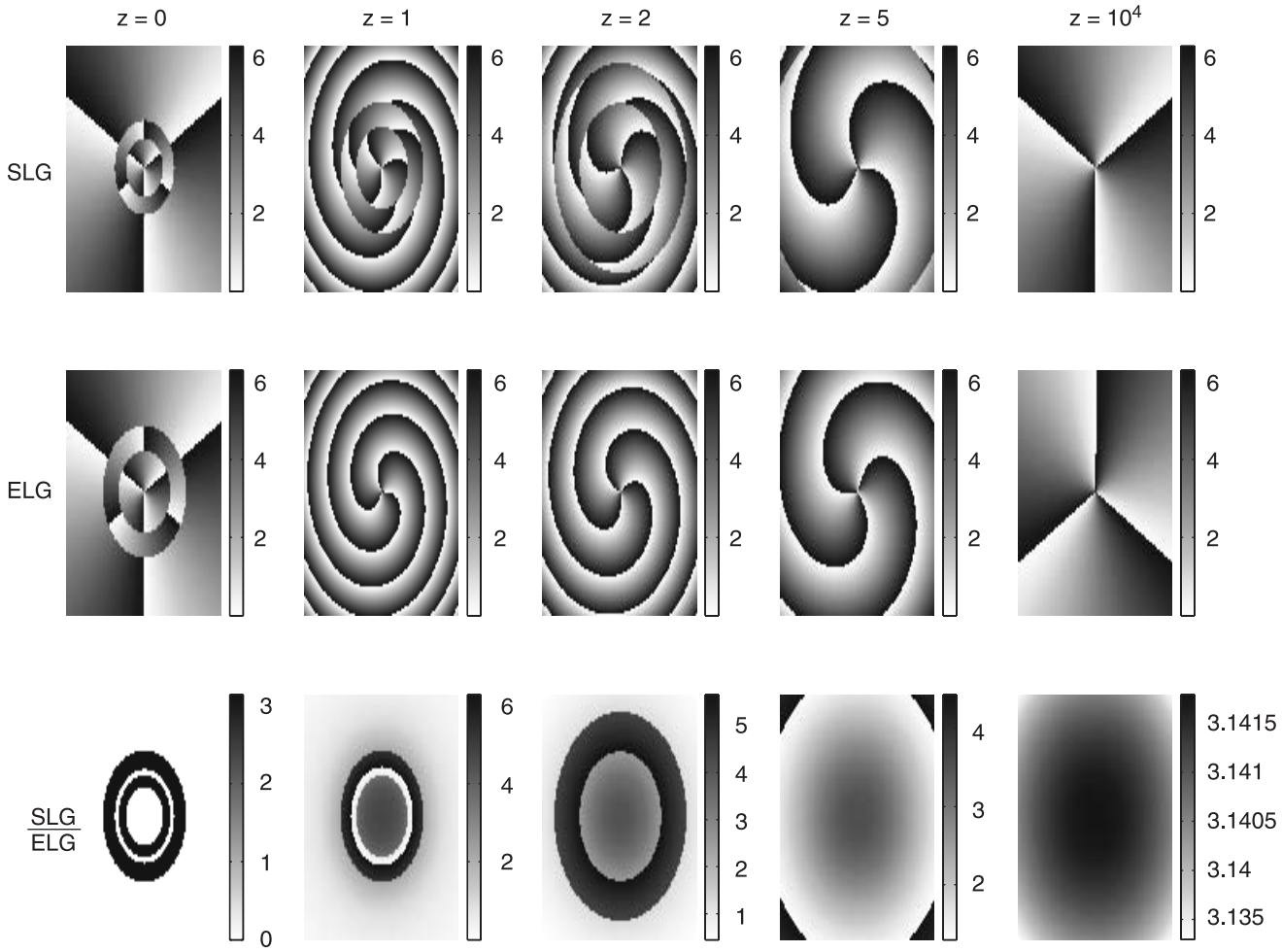

Fig. 9. Phase distribution in the transverse plane $(\tilde{x},\tilde{y})$ of $\phi_{nm}^{SLG}(\tilde{x},\tilde{y},\tilde{z})$ (first line), $\phi_{nm}^{ELG}(\tilde{x},\tilde{y},\tilde{z})$ (second line) and $\phi_{nm}^{SLG}(\tilde{x},\tilde{y},\tilde{z})/\phi_{nm}^{ELG}(\tilde{x},\tilde{y},\tilde{z})$ (third line) for $n = 5$, $m = 2$ at different $\tilde{z}$ positions: from the beam waist ($\tilde{z} = 0$) to the far-field ($\tilde{z} = 10^4$). We have set the argument to be between $[0,2\pi]$. For the first two lines, the white color stands for 0.

So, there is no difference between arguments of Laguerre functions in the far field; both of them – standard and elegant – are zero. For this reason, the only relevant factors which contribute to the phase difference between standard and elegant LG beam fields are $[v(\tilde{z})^*/v(\tilde{z})]^{n+m}$, and $[1/v(\tilde{z})]^{2n}$ respectively. Therefore, the global difference of phase between these two types of beams in the far field finally is:

$$\Delta_{SEL} = \arg_{SL} - \arg_{EL} = -(\min(n,m))\,\pi/2. \qquad (17)$$

In this way, the differences in azimuthal phase discontinuity orientations of both beams are strictly defined in the far field. They are equal $-\pi/2$ in Fig. 8 and $-\pi$ in Fig. 9. The radial index of SLG and ELG beams differentiates quantitatively the phase transverse distribution of these beams as they are seen in the far-field.

5. Conclusions

In this communication, we have proved and numerically verified that the diagonal relations between standard beams can be directly extended to elegant beams. The explicit diagonal relations (15) and (16) given here for elegant beams do not seem to have been reported earlier.

We have also presented preliminary results concerning evolution of transverse phase distribution of elegant beam fields. This issue also has not been much explored in the literature yet. Differences in the phase discontinuity locations between beams of both types, and their evolution during propagation, depend on radial indices of Laguerre functions describing the beams. We have shown that at the waist and in the far-field the phase portraits obtained are well defined and are simple enough to be quantitatively interpreted. In the range between these two limits the phase portraits are of more complicated form and depend on all parameters of the beams.

Appendix

Derivation of the relation between the diagonal EHG and non-diagonal EHG (Eq. 15) beams is presented below. We start from the relation between the Hermite function in a form given by Abramochkin *et al*. and Allen *et al*. [6,7]:

$$\sum_{k=0}^{n+m}(-2)^k P_k^{(n-k,m-k)}(0)H_{n+m-k}(x)H_k(y) = (\sqrt{2})^{n+m}H_n\left(\frac{x-y}{\sqrt{2}}\right)H_m\left(\frac{x+y}{\sqrt{2}}\right), \tag{A.1}$$

which is valid for both real and complex x and y arguments. Applying to eq. A.18 the definition of Hermite polynomials:

$$H_n(x) = \sum_{k=0}^{[n/2]}\frac{(-1)^k n!(2x)^{n-2k}}{k!(n-2k)!} \tag{A.2}$$

yields for $N = n + m$:

$$\sum_{k=0}^{N}(-2)^k P_k^{(n-k,m-k)}(0)\left(\sum_{l=0}^{[(N-k)/2]}\frac{(-1)^l(N-k)!(2x)^{N-k-2l}}{l!(N-k-2l)!}\right)\left(\sum_{j=0}^{[k/2]}\frac{(-1)^j k!(2y)^{k-2j}}{j!(k-2j)!}\right) =$$
$$(\sqrt{2})^{n+m}\left(\sum_{j=0}^{[n/2]}\frac{(-1)^j n!(2(x-y)/\sqrt{2})^{n-2j}}{j!(n-2j)!}\right)\left(\sum_{l=0}^{[m/2]}\frac{(-1)^l m!(2(x+y)/\sqrt{2})^{m-2l}}{l!(m-2l)}\right)$$

By developing the summation:

$$\sum_{k=0}^{N}\sum_{j=0}^{[(N-k)/2]}\sum_{l=0}^{[k/2]}(-2)^k P_k^{(n-k,m-k)}(0)\frac{(-1)^l(N-k)!(2x)^{N-k-2l}}{l!(N-k-2l)!}\frac{(-1)^j k!(2y)^{k-2j}}{j!(k-2j)!} =$$
$$(\sqrt{2})^{n+m}\sum_{l=0}^{[n/2]}\sum_{j=0}^{[m/2]}\frac{(-1)^l n!}{l!(n-2l)!}\frac{(-1)^j m!}{j!(m-2j)!}\left(\frac{2(x-y)}{\sqrt{2}}\right)^{n-2l}\left(\frac{2(x+y)}{\sqrt{2}}\right)^{m-2j}$$

and by multiplying each term of these summations by $\kappa^{N-2j-2l}$ where $\kappa \neq 0$ is an arbitrary, eventually complex, parameter, the above equation can be rewritten as:

$$\sum_{k=0}^{N}\sum_{j=0}^{[(N-k)/2]}\sum_{l=0}^{[k/2]}(-2)^k P_k^{(n-k,m-k)}(0)\frac{(-1)^l(N-k)!(2x)^{N-k-2l}}{l!(N-k-2l)!}\frac{(-1)^j k!(2y)^{k-2j}}{j!(k-2j)!}\kappa^{N-2j-2l} =$$
$$(\sqrt{2})^{n+m}\sum_{l=0}^{[n/2]}\sum_{j=0}^{[m/2]}\frac{(-1)^l n!}{l!(n-2l)!}\frac{(-1)^j m!}{j!(m-2j)!}\left(\frac{2(x-y)}{\sqrt{2}}\right)^{n-2l}\left(\frac{2(x+y)}{\sqrt{2}}\right)^{m-2j}\kappa^{N-2j-2l}$$

Since $\kappa^{N-2j-2l} = \kappa^{N-k-2j+k-2l}$, we get:

$$\sum_{k=0}^{N}\sum_{j=0}^{[(N-k)/2]}\sum_{l=0}^{[k/2]}(-2)^k P_k^{(n-k,m-k)}(0)\frac{(-1)^l(N-k)!(2x\kappa)^{N-k-2l}}{l!(N-k-2l)!}\frac{(-1)^j k!(2y\kappa)^{k-2j}}{j!(k-2j)!} =$$
$$(\sqrt{2})^{n+m}\sum_{l=0}^{[n/2]}\sum_{j=0}^{[m/2]}\frac{(-1)^l n!}{l!(n-2l)!}\frac{(-1)^j m!}{j!(m-2j)!}\left(\frac{2(x-y)\kappa}{\sqrt{2}}\right)^{n-2l}\left(\frac{2(x+y)\kappa}{\sqrt{2}}\right)^{m-2j}$$

or equivalently

$$\sum_{k=0}^{N}(-2)^k P_k^{(n-k,m-k)}(0)H_{N-k}(\kappa x)H_k(\kappa y) = (\sqrt{2})^{n+m}H_n\left(\frac{\kappa(x-y)}{\sqrt{2}}\right)H_m\left(\frac{\kappa(x+y)}{\sqrt{2}}\right) \tag{A.3}$$

Then we set $\kappa = 1/v(\tilde{z})$ and multiply each side of Eq. (A.3) by

$$2^{-\frac{n+m}{2}}\sqrt{\frac{2}{n!m!\pi}}\left(\frac{1}{v(\tilde{z})}\right)^{n+m}G(\tilde{x},\tilde{y},\tilde{z})$$

That finally reads, accordingly to the notation of Eq. (15)

$$\sum_{k=0}^{N}(-2)^k P_k^{(n-k,m-k)}(0)\sqrt{\frac{(n+m-k)!k!}{n!m!}}\psi_{N-k,k}^{EHG}(\tilde{x},\tilde{y},\tilde{z}) = 2^{\frac{n+m}{2}}\psi_{n,m}^{EHG}\left(\frac{\tilde{x}-\tilde{y}}{\sqrt{2}},\frac{\tilde{x}+\tilde{y}}{\sqrt{2}},\tilde{z}\right) \tag{A.4}$$

The parallel relation for elegant Laguerre-Gaussian beams (eq. 16) can be proved by use of considerations similar to those employed by Zauderer [14] in another context, or along the lines presented in the work, where the following relation [6,7]:

$$\sum_{k=0}^{N}(2i)^k P_k^{(n-k,m-k)}(0)H_{N-k}(x)H_k(y) = \tag{A.5}$$
$$2^{n+m}\begin{cases}(-1)^m m!(x+iy)^{n-m}L_m^{n-m}(x^2+y^2) & \text{for } n \geq m\\ (-1)^n n!(x-iy)^{m-n}L_n^{m-n}(x^2+y^2) & \text{for } n \leq m\end{cases}$$

can be treated as a starting point of such analysis.

References

1. H. Kogelnik and T. Li, *Appl. Opt.* **5**, 1550 (1966).
2. A.E. Siegman, *Lasers* (Mill Valley California, 1986).
3. A.E. Siegman, *J. Opt. Soc. Am.* **63**, 1093 (1973).
4. R. Pratesi and L. Ronchi, *J. Opt. Soc. Am.* **67**, 1274 (1977).
5. S. Saghafi, C.J.R. Sheppard, and J.A. Piper, *Optics Commun.* **191**, 173 (2001).
6. E. Abramochkin and V. Volostnikov, *Optics Commun.* **83**, 123 (1991).
7. L. Allen, M.W. Beijersbergen, R.J.C. Spreeuw, and J.P. Woerdman, *Phys. Rev.* A **45**, 8185 (1992).
8. L. Allen, M. Padgett, and M. Babiker, *Prog. Opt.* **39**, 291 (1999).
9. S. Saghafi and C.J.R. Sheppard, *Optics Commun.* **153**, 207 (1998).
10. M.W. Beijersbergen, L. Allen, H.E.L.O. Van Der Veen, and J. Woerdman, *Optics Commun.* **96**, 123 (1993).
11. S. Saghafi and C.J. R. Sheppard, *J. Mod. Opt.* **45**, 1999 (1998).
12. B. Lü and H. Ma, *Optics Commun.* **174**, 99 (2000).
13. T. Takenaka, M. Yokota, and O. Fukumitsu, *J. Opt. Soc. Am.* A **2**, 826 (1985).
14. E. Zauderer, *J. Opt. Soc. Am.* A **3**, 465 (1986).

